

# Structural Behavior of Incomplete Box Girder Bridges Subjected to Unpredicted Loads

E. H. N. Gashti, J. Razzaghi, K. Kujala

**Abstract**—In general, codes and regulations consider seismic loads only for completed structures of the bridges while, evaluation of incomplete structure of bridges, especially those constructed by free cantilever method, under these loads is also of great importance. Hence, this research tried to study the behavior of incomplete structure of common bridge type (box girder bridge), in construction phase under vertical seismic loads. Subsequently, the paper provided suitable guidelines and solutions to resist this destructive phenomenon. Research results proved that use of preventive methods can significantly reduce the stresses resulted from vertical seismic loads in box cross sections to an acceptable range recommended by design codes.

**Keywords**—Box girder bridges, Prestress loads, Free cantilever method, Seismic loads, Construction phase.

## I. INTRODUCTION

BRIDGES are considered of important structures in all countries, therefore, their design and construction demand serious efforts and attentions. It is observed that in different codes [1]-[3], regulations consider seismic loads only for the completed structures of bridges while, such structures can also be under danger of earthquake happening in phase of construction. This issue can be noted more significantly for bridges with large spans and more vulnerable to seismic loads.

In this research it was tried to take into account the incomplete structure of a box girder bridge constructed with free-cantilever method subjected to vertical seismic loads. For analysis purpose, a prestressed concrete deck of a real box girder bridge constructed at north of Iran was selected for simulation. The recently constructed bridge was selected for analysis because of its location which is in a region with high risk of seismic hazard, and also the large spans of bridge deck. For evaluation, the internal forces in different cross sections of box girders resulted from deck structure weight and prestress loads were calculated during construction phase, firstly. These design forces were then added to the forces resulted from seismic loads in construction phase and eventually compared with permitted stresses ranges specified in reliable codes. Subsequently, guidelines and solutions to reduce seismic-induced stresses were suggested. Research results indicated

E. H. N. Gashti is with the Faculty of Technology, University of Oulu, FI - 90014 Finland (phone: +358 (0) - 417- 248- 344; e-mail: Ehsan.hassani@oulu.fi).

J. Razzaghi is with the Department of Civil Engineering, The University of Guilan, Rasht 41635-3756 Iran (phone: +98-131-669-0270; e-mail: Javadr@guilan.ac.ir).

K. Kujala is with the Faculty of Technology, University of Oulu, FI - 90014 Finland (phone: +358 (0) - 405- 456- 930; e-mail: Kauko.kujala@oulu.fi).

that use of these solutions can reduce seismic stresses significantly and prevent destruction of bridge deck under vertical seismic effects.

## II. BRIDGE STRUCTURE SPECIFICATIONS

The structure taken into account in this research is related to a prestressed concrete bridge deck with box segments which is constructed with free-cantilever method at north of Iran, shown in Fig. 1. The bridge includes 4 spans from which the longest one is 125 m located at middle of spans. This span has 28 segments with length of 4.15 m, 2 segments with 3.55 m and the key segment with 1.7 m length.



Fig. 1 Box bridge constructed by free-cantilever method in study

Longitudinal situation of bridge is shown in Fig. 2. In Fig. 3 the cross section of segments in all connection slits is shown. It is further explained that dimensions A, B and C differ along the bridge span.

## III. SPECIFICATIONS OF SECTIONS AND MATERIALS

Ultimate strength of each prestressed strand used in bridge deck was selected as 26 ton. As a result, the ultimate strength of each 12 strands cable was calculated as 312 ton and prestress force of cables was assumed as 75% ultimate strength equal to 238 ton according to detailed construction plans.

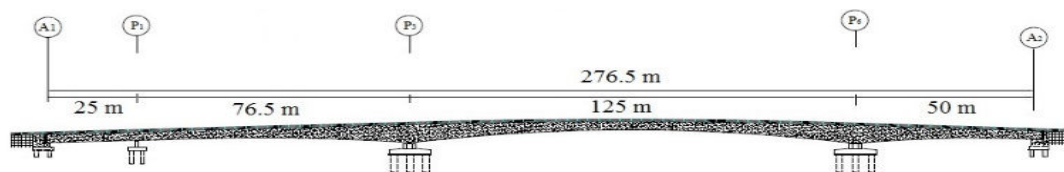


Fig. 2 Longitudinal situation of the bridge and location of spans

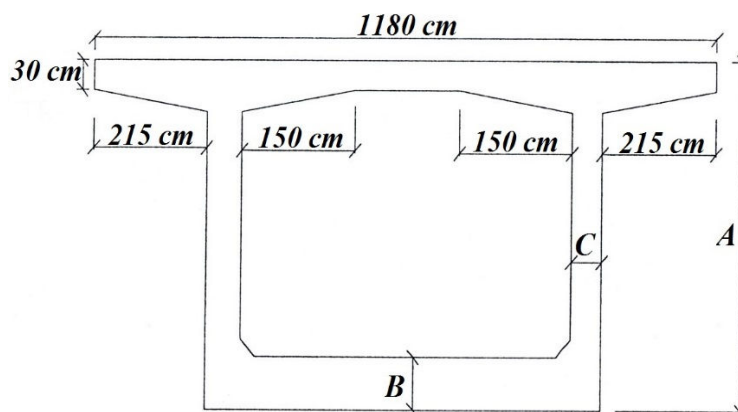


Fig. 3 General cross section of spans in connection slits

It is also explained that  $f_c$  (ultimate strength of 28 days concrete) in bridge deck is equal to  $400 \text{ kg/cm}^2$ . Permitted stresses of concrete used in bridge deck according to AASHTO code are calculated as following [1]:

Permitted compressive stress:

$$0.4 \cdot f_c = -0.4 \times 400 \left( \frac{\text{kg}}{\text{cm}^2} \right) = -160 \left( \frac{\text{kg}}{\text{cm}^2} \right) \quad (1)$$

Permitted tensile stress:

$$0.4 \times 2 \sqrt{f_c} = 16 \left( \frac{\text{kg}}{\text{cm}^2} \right) \quad (2)$$

It is explained that in foregoing equations the unit of  $f_c$  is defined as  $(\text{kg/cm}^2)$ .

Critical sections specifications (connection slits) are according to the values shown in Table I. Owing to the symmetry of decks construction around pile  $P_3$  shown in Fig. 4, specifications of slits at right side of pile are as same as the left ones.

#### IV. BRIDGE DECK SIMULATION AND CALCULATION OF INTERNAL STRESSES

Bridge deck was simulated using SAP2000 software [4] and regarding structural and geometrical specifications of

segments and materials used as well as detailed plans available for construction. After simulation of bridge deck in free-cantilever method, the internal forces were calculated. In this research the middle pile  $P_3$  with 14 segments in each free-cantilever wings, at right and left sides was selected as benchmark. It is further explained that during the construction of deck and after installation of 7<sup>th</sup> segment, one temporary pile is constructed only in one side of cantilever wings to avoid structure reversal resulted from decks gravity loads, shown in Fig. 4.

It is further explained that this temporary pile and bridge deck is not connected to each other and a predefined distance around 10 cm is defined between them. This distance is to avoid deck and temporary pile contact during installation of next segments and further displacements resulted in deck (segments 7<sup>th</sup> to 14<sup>th</sup>).

In Fig. 5 the prestressed bridge deck after installation of all segments is shown.

In this study load combination of Dead+Prestress is introduced as Combo1. In Figs. 6, 7 internal forces resulted from this load combination are shown.

TABLE I  
GEOMETRIC SPECIFICATIONS OF CRITICAL CROSS SECTIONS

| Geometric Specifications                             | Cross Sections |       |       |       |       |       |       |       |
|--|----------------|-------|-------|-------|-------|-------|-------|-------|
|  | 1R             | 3R    | 5R    | 7R    | 9R    | 11R   | 13R   | 15R   |
| Height (m)   | 6.18           | 5.57  | 4.94  | 4.42  | 4.02  | 3.73  | 3.56  | 3.5   |
| A (Cross section area) ( $\text{m}^2$ )              | 15.15          | 13.24 | 10.98 | 10.14 | 9.74  | 9.45  | 9.28  | 9.23  |
| C1 (Distance between uppermost and neutral axes) (m) | 3.62           | 2.78  | 2.16  | 1.85  | 1.68  | 1.55  | 1.48  | 1.39  |
| C2 (Distance between lowermost and neutral axes) (m) | 2.92           | 2.79  | 2.78  | 2.57  | 2.34  | 2.18  | 2.11  | 2.08  |
| Ixx (Moment of inertia) ( $\text{m}^4$ )             | 104.6          | 71.2  | 45.03 | 32.22 | 25.12 | 21.96 | 19.66 | 19.04 |
| Ax (Area of web) ( $\text{m}^2$ )                    | 6.34           | 4.47  | 4.09  | 3.62  | 3.22  | 2.93  | 2.76  | 2.71  |

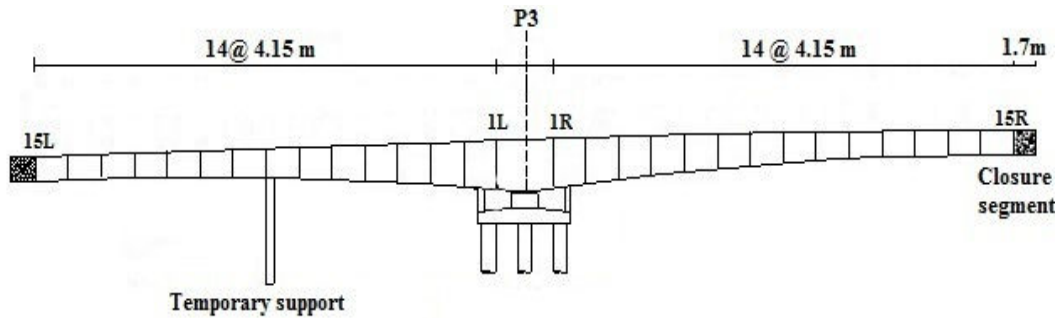


Fig. 4 Middle pile P3 with 14 segmental decks in each side and installation of temporary pile after segment 7th

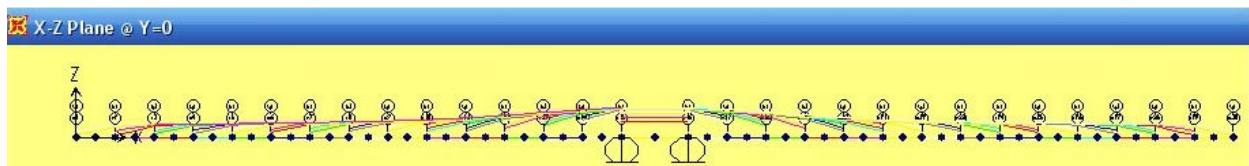


Fig. 5 Prestressed bridge deck simulation after installation with 14 segments

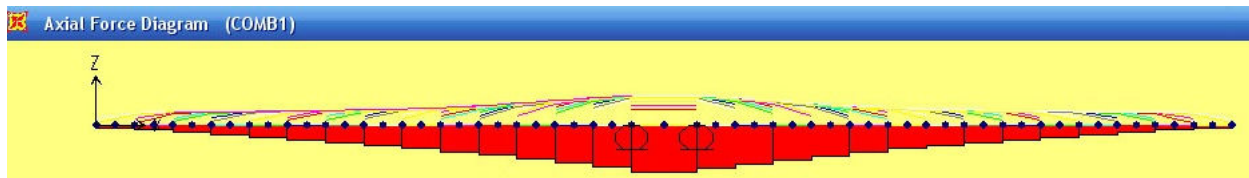


Fig. 6 Axial forces resulted from load combination Combo1 after installation of segment 14th

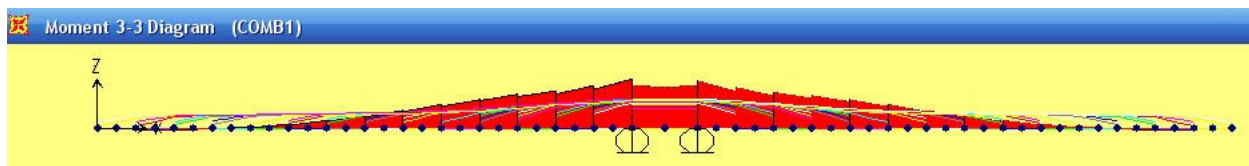


Fig. 7 Bending moment M3-3 resulted from load combination Combo1 after installation of segment 14th

For calculation of stresses in this structure and owing to the symmetry of decks at right and left sides of pile P<sub>3</sub>, the deck on right side was selected as benchmark for taking into analysis. For analysis of segmental box girders and according to the PCI instructions; no tensile stress is allowed at the top of connection slits neither in construction phase nor in service phase [5]. For calculation of stresses under load combination Combo1, following equations are used:

$$\text{Stress in uppermost axis } f_1 = -\frac{F_e}{A_g} - \frac{M.C_1}{I_g} \quad (3)$$

$$\text{Stress in lowermost axis } f_2 = -\frac{F_e}{A_g} + \frac{M.C_2}{I_g} \quad (4)$$

where  $F_e$  is prestress force and  $C_1$  &  $C_2$  are distances between uppermost and lowermost axes from neutral axis in deck cross section, respectively.  $M$  is equal to  $M_{(Dead)} + M_{(Prestress)}$  (summation of bending moments resulted from dead loads and prestress forces).  $A_g$  is cross section area and  $I_g$  is moment of inertia.

In Tables II–IV values of internal forces and stresses resulted from load combination Combo1 at every other slits after installation of 10<sup>th</sup>, 12<sup>th</sup> and 14<sup>th</sup> segments are shown. It is further explained that in box bridges and after installation of each segment, the force distributions in connection slits change.

TABLE II  
AXIAL FORCES, BENDING MOMENTS AND STRESSES RESULTED FROM COMBO1 AT DIFFERENT SLITS AFTER INSTALLATION OF 10<sup>th</sup> SEGMENT

| Forces and Stresses                            | Section Number |       |       |       |      |
|--|----------------|-------|-------|-------|------|
|  | 1R             | 3R    | 5R    | 7R    | 9R   |
| Compressive axial force (ton)                  | -5842          | -4465 | -3062 | -1885 | -938 |
| Bending moment M <sub>3-3</sub> (ton.m)        | -4008          | -2079 | -1460 | -126  | 576  |
| Stress at uppermost axis (kg/cm <sup>2</sup> ) | -25            | -26   | -21   | -18   | -13  |
| Stress at lowermost axis (kg/cm <sup>2</sup> ) | -50            | -42   | -37   | -20   | -4   |

TABLE III  
AXIAL FORCES, BENDING MOMENTS AND STRESSES RESULTED FROM COMBO1 AT DIFFERENT SLITS AFTER INSTALLATION OF 12<sup>TH</sup> SEGMENT

| Forces and Stresses                            | Section Number |       |       |       |       |      |
|--|----------------|-------|-------|-------|-------|------|
|  | 1R             | 3R    | 5R    | 7R    | 9R    | 11R  |
| Compressive axial force (ton)                  | -6791          | -5411 | -4011 | -2835 | -1887 | -467 |
| Bending moment M <sub>3,3</sub> (ton.m)        | -9783          | -6719 | -5087 | -2451 | -313  | 522  |
| Stress at uppermost axis (kg/cm <sup>2</sup> ) | -11            | -15   | -12   | -14   | -17   | -9   |
| Stress at lowermost axis (kg/cm <sup>2</sup> ) | -72            | -67   | -68   | -48   | -22   | 0.2  |

TABLE IV  
AXIAL FORCES, BENDING MOMENTS AND STRESSES RESULTED FROM COMBO1 AT DIFFERENT SLITS AFTER INSTALLATION OF 14<sup>TH</sup> SEGMENT

| Forces and Stresses                            | Section Number |        |        |       |       |       |      |
|--|----------------|--------|--------|-------|-------|-------|------|
|  | 1R             | 3R     | 5R     | 7R    | 9R    | 11R   | 13R  |
| Compressive axial force (ton)                  | -7737          | -6356  | -4957  | -3782 | -2835 | -1888 | -937 |
| Bending moment M <sub>3,3</sub> (ton.m)        | -17055         | -12854 | -10228 | -6307 | -2755 | -466  | 460  |
| Stress at uppermost axis (kg/cm <sup>2</sup> ) | 8              | 2      | 4      | -1    | -1    | -17   | -14  |
| Stress at lowermost axis (kg/cm <sup>2</sup> ) | -99            | -98    | -108   | -88   | -54   | -25   | -52  |

### V. CALCULATION OF VERTICAL SEISMIC LOADS AND STRESSES RESULTED IN DECK CONNECTION SLITS

In order to compute vertical seismic loads for the free-cantilever deck, fundamental period of vibration is calculated at first [6].

$$T = 2\pi \sqrt{\frac{\sum P_i X_i^2}{g \sum P_i X_i}} \quad (5)$$

where  $P_i$  (ton) is weight of segments,  $X_i$  (m) is displacements resulted from segments weight and  $g$  is gravity acceleration ( $m/s^2$ ).

If fundamental period of vibration calculated from (5) for free-cantilever deck is less than 0.5 (s), static force method and else, dynamic analysis method are selected [6], [7].

For calculation of vertical seismic loads using static force method, following equations are utilized [6]-[8]:

$$V = C.W \quad (6)$$

where  $V$  is base-shear,  $C$  is earthquake coefficient and  $W$  is the total weight of deck segments.

$$c = \frac{AB I}{R} \quad (7)$$

where  $A$  peak ground acceleration by considering the zone with high risk is equal to 0.3,  $B$  is spectral constant,  $I$  importance coefficient which regarding the medium importance of structure is selected as 1 and  $R$  response

modification factor regarding the cantilever coefficient of deck is equal to 4.

Spectral constant  $B$  regarding the soil coefficient and seismic zone is computed by considering (8) and (9).

$$0 \leq T \leq T_0 \Rightarrow B = 1 + S\left(\frac{T}{T_0}\right) \quad (8)$$

$$T_0 \leq T \leq T_s \Rightarrow B = S + 1 \quad (9)$$

In above equations regarding the soil coefficient (very humid) and seismic zone (high risk) the values of parameters  $T_0$ ,  $T_s$  and  $S$  are considered as 0.15, 1 and 1.75, respectively.

To calculate base-shear distribution along the cantilever deck (10) is used as following:

$$\text{Vertical seismic force in segment } i \quad F_i = V \times \frac{W_i h_i}{\sum_{j=1}^n W_j h_j} \quad (10)$$

where  $W$  is weight if each segment,  $V$  is base-shear and  $h$  is distance between segments and base-segment over the pile.

For calculation of vertical seismic loads of 10 segmental installation, static force method was used regarding the fundamental period of vibration less than 0.5 S and for 12 and 14 segmental installations, spectrum analysis method was selected using SAP2000 software (fundamental period of vibration more than 0.5 S).

Internal seismic forces available in connection slits resulted from vertical seismic loads distributed along cantilever deck for 10, 12, and 14 segmental installations are shown in Figs. 8-10.

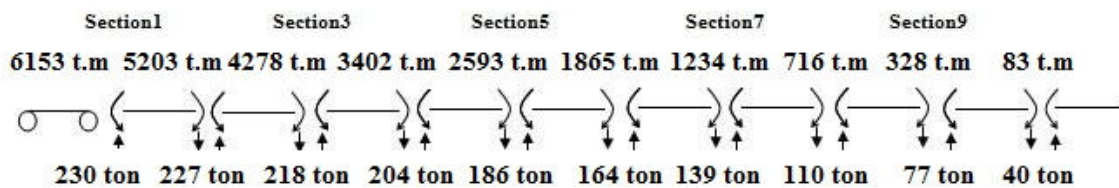


Fig. 8 Internal forces resulted from vertical seismic loads with installation of segment 10th (ton)

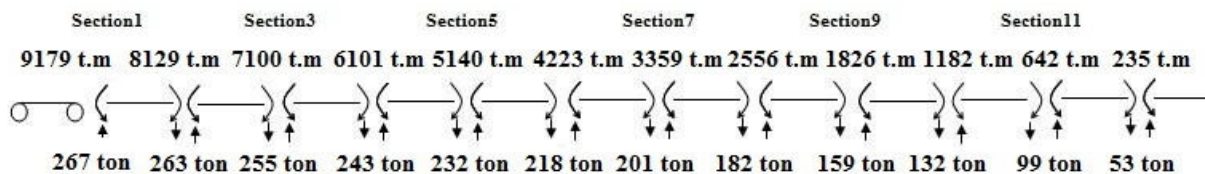


Fig. 9 Internal forces resulted from vertical seismic loads with installation of segment 12th (ton)

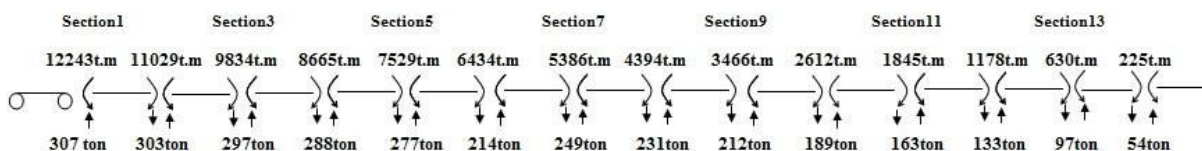


Fig. 10 Internal forces resulted from vertical seismic loads with installation of segment 14th (ton)

### VI. RESULTS AND DISCUSSION

The stresses resulted from vertical seismic loads and their combinations with stresses generated from Combo1 (presented

previously in Tables II-IV) are shown in Tables V-VII. It is added that in these tables EQZN and EQZP denote downward and upward seismic loads, respectively.

TABLE V  
BENDING STRESSES RESULTED FROM SEISMIC LOADS AND THEIR COMBINATION WITH DEAD AND PRESTRESS LOADS WITH 10 SEGMENTAL INSTALLATION (KG/CM<sup>2</sup>)

| Stresses                               | Section Number |     |     |     |     |
|--|----------------|-----|-----|-----|-----|
|  | 1R             | 3R  | 5R  | 7R  | 9R  |
| Stress at uppermost axis (EQZN)        | 21             | 17  | 12  | 7   | 2   |
| Stress at uppermost axis (Combo1+EQZN) | -3             | -9  | -8  | -11 | -11 |
| Stress at uppermost axis (Combo1+EQZP) | -46            | -42 | -33 | -25 | -16 |
| Stress at lowermost axis (EQZN)        | -17            | -17 | -16 | -10 | -3  |
| Stress at lowermost axis (Combo1+EQZN) | -67            | -59 | -53 | -29 | -7  |
| Stress at lowermost axis (Combo1+EQZP) | -33            | -25 | -21 | -10 | -1  |

TABLE VI  
BENDING STRESSES RESULTED FROM SEISMIC LOADS AND THEIR COMBINATION WITH DEAD AND PRESTRESS LOADS WITH 12 SEGMENTAL INSTALLATION (KG/CM<sup>2</sup>)

| Stresses                               | Section Number |     |      |     |     |      |
|--|----------------|-----|------|-----|-----|------|
|  | 1R             | 3R  | 5R   | 7R  | 9R  | 11R  |
| Stress at uppermost axis (EQZN)        | 32             | 28  | 25   | 19  | 12  | 5    |
| Stress at uppermost axis (Combo1+EQZN) | 21*            | 13* | 13*  | 6*  | -5  | -4   |
| Stress at uppermost axis (Combo1+EQZP) | -51            | -42 | -37  | -33 | -29 | -13  |
| Stress at lowermost axis (EQZN)        | -26            | -28 | -32  | -27 | -17 | -6   |
| Stress at lowermost axis (Combo1+EQZN) | -98            | -95 | -100 | -74 | -39 | -6   |
| Stress at lowermost axis (Combo1+EQZP) | -47            | -39 | -36  | -21 | -5  | 6<16 |

TABLE VII  
BENDING STRESSES RESULTED FROM SEISMIC LOADS AND THEIR COMBINATION WITH DEAD AND PRESTRESS LOADS WITH 14 SEGMENTAL INSTALLATION (KG/CM<sup>2</sup>)

| Stresses                               | Section Number |      |      |      |     |     |     |
|--|----------------|------|------|------|-----|-----|-----|
|  | 1R             | 3R   | 5R   | 7R   | 9R  | 11R | 13R |
| Stress at uppermost axis (EQZN)        | 42             | 39   | 37   | 32   | 24  | 14  | 5   |
| Stress at uppermost axis (Combo1+EQZN) | 50*            | 41*  | 41*  | 31*  | 13* | -3  | -8  |
| Stress at uppermost axis (Combo1+EQZP) | -34            | -37  | -33  | -33  | -35 | -30 | -19 |
| Stress at lowermost axis (EQZN)        | -34            | -39  | -28  | -20  | -12 | -6  | -2  |
| Stress at lowermost axis (Combo1+EQZN) | -133           | -137 | -136 | -107 | -67 | -31 | -7  |
| Stress at lowermost axis (Combo1+EQZP) | -64            | -59  | -81  | -68  | -43 | -18 | -3  |

As it is observed from Tables V-VII and by considering (1) and (2), all tensile and compressive stresses at the bottom of connection slits under Combo1+EQZ(N & P) are in permitted range of codes. It is also observed that according to (2) and PCI recommendation that no tensile stress was allowed at the

top of connection slits, after installation of segment 12th, stresses resulted from Combo1+EQZN at the top of slits 1-9 have become tensile and in some slits have exceeded from permitted range. These stresses are highlighted with \* sign in tables. As a consequent, attention to this issue concerning

deduction these stresses resulted from vertical downward seismic loads seems to be of great importance.

In order to reduce stresses resulted from vertical downward seismic load, two general solutions are suggested. The first one is introduced as changing in geometrical specifications of box sections in the way that in all processes of segments installations no tensile stress happens. This solution can result in a significant increase in construction expenses of bridge deck regarding its effect on the whole deck length.

The second solution is presented in order to reduce the values of vertical seismic loads using supportive temporary piles which will be installed under cantilever deck during the construction. The connection of these temporary piles with cantilever deck is in the way that they will work as an extra support to take only vertical seismic loads without any resistance in front of deck displacements resulted from segments installations. A suggested detailed plan for this solution is presented in Fig. 11. The ability of this connection movement using flexible bolts and plates, induces no extra stresses resulted from pile resistance in front of deck displacements under segments installations.

It is obvious that design of bolts, connection plates, and distances between holes is of great importance and use of these details or any similar one requires extensive theoretical and experimental researches.

To calculate seismic loads for the part of deck with free-cantilever behavior (after temporary pile) static force method explained in former parts is used and for the part between main pile and temporary pile following method is utilized [9].

Following parameters are used for uniformly distributed loading ( $P_0$ ) which results in displacement  $V_s(x)$  along the bridge deck:

$$\alpha = \int_0^l V_s(x) \cdot dx \quad (11)$$

$$\beta = \int_0^l W(x) \cdot V_s(x) \cdot dx \quad (12)$$

$$\gamma = \int_0^l W_x \cdot V_s^2(x) \cdot dx \quad (13)$$

$$T = 2\pi \sqrt{\frac{\gamma}{P_0 a g}} \quad (14)$$

where  $W(x)$  is unit of length weight,  $V_s(x)$  is displacements of deck under applying uniformly distributed loading ( $P_0$ ) and  $T$  is fundamental period of vibration. Lastly, using (15) the effective seismic load available in each section is determined as following:

$$P(x) = \frac{\beta \cdot C}{\gamma} W(x) \cdot V_s(x) \quad (15)$$

where  $C$  is earthquake coefficient which was calculated according to conservative assumption 4 for response modification factor and (7).

In Table VIII, stresses resulted from seismic loads EQZN after installation of supportive temporary pile and their combination with stresses generated from Combo1 after construction of segment 14<sup>th</sup> are shown and compared with recommendation values of codes.

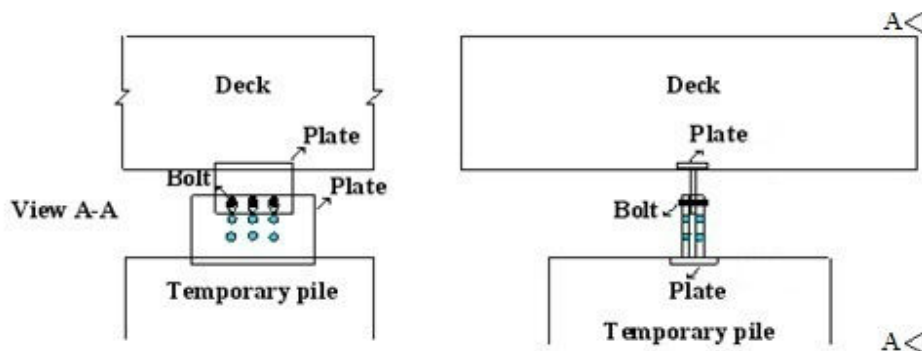


Fig. 11 Connection details of supportive temporary pile and deck

TABLE VIII  
STRESSES RESULTED FROM VERTICAL SEISMIC LOADS AFTER INSTALLATION OF SUPPORTIVE TEMPORARY PILE (KG/CM<sup>2</sup>)

| Stresses                               | Section Number |     |      |      |     |     |     |
|--|----------------|-----|------|------|-----|-----|-----|
|  | 1R             | 3R  | 5R   | 7R   | 9R  | 11R | 13R |
| Stress at uppermost axis (Combo1+EQZN) | 6              | 2   | 7    | 10   | 3   | -9  | -11 |
| Stress at lowermost axis (Combo1+EQZN) | -97            | -98 | -113 | -103 | -74 | -35 | -8  |

As it can be extracted from the Table VIII, stresses were reduced significantly (70%-90%) after installation of supportive temporary pile.

## VII. CONCLUSION

Regarding the unpredictability of earthquakes happening times, bridges made by free cantilever method with long spans can be vulnerable in front of seismic loads during construction phase. Whereas the regulations and codes have been unclear about incomplete structure behavior of bridges during

construction phase, performing theoretical and experimental researches and suggestion of recommendations for further clarity of this issue seems to be of great importance. In this study a real box girder bridge constructed at north of country Iran was simulated in construction phase and possible problems for incomplete structure of bridge deck were highlighted. The research was further extended to introduce solutions in deduction of extra seismic stresses and eventually, the results were compared with values without using these solutions and their differences were highlighted.

#### REFERENCES

- [1] AASHTO LRFD Bridge design specifications, American Association of High way and Transportation officials, Washington D.C., 1994.
- [2] EC 8. 1994a. Euro Code8 – Design Provisions for Earthquake Resistance of Structures – Part 1-1: General Rules – Seismic Actions and General Requirements for Structures – European Prestandard ENV 1998-1-1.
- [3] EC 8. 1994b. Euro Code8 – Design Provisions for Earthquake Resistance of Structures – Part 2: Bridges - European Prestandard ENV 1998-2.
- [4] Sap2000, Advanced 10.0.1, Structural Analysis Program.
- [5] PCI Bridge Producers Committee, “Recommended Composite Bridge deck Panels”, PCI Journal, V.33, No.2, March-April 1998, PP.67-109.
- [6] Moghaddam, H. Earthquake Engineering, fundamentals and application, Tehran. Farhang Pub, 2002.
- [7] Transportaion, Federal highway administration. U.S. Department of Post-Earthquake Reconnaissance Report on Transportation Infrastructure: Impact of the February 27, 2010, Offshore Maule Earthquake in Chile. Offshore Maule Earthquake in Chile : Publication Number: FHWA-HRT-11-030.
- [8] Gupta, A.K. Response Spectrum Method. In seismic analysis and design of structures. 1992 by CRC Press.
- [9] Road and Railway Bridges Seismic Resistant Design Code. No:463. Ministry of Roads and Transportation, Tehran, 2008.